

# The Influence of Oscillator Behavior on Accumulated Phase Error during Dynamic Environmental Conditions

Mike F. Wacker

Vectron International, Mount Holly Springs, Pennsylvania, USA

[mwacker@vectron.com](mailto:mwacker@vectron.com)

Peter Matthews

Vectron International, Hudson, New Hampshire, USA

[pmatthews@vectron.com](mailto:pmatthews@vectron.com)

## Abstract

*This paper examines the phase error that can occur in telecommunication systems during exposure of oven controlled crystal oscillators (OCXO) to various airflow scenarios in open-loop or closed-loop operation. The objective is to make system designers aware of largely undocumented and unadvertised OCXO behavioral characteristics. With this knowledge, the designer is better able to anticipate and successfully solve problematic timing issues.*

## I. Introduction

Today's communication systems are built upon architectures that demand timing strategies exhibiting both accurate and reliable frequency or phase characteristics. In most implementations, a timing signal is either embedded within the data stream or received from a separate carrier, e.g., GPS. Within the system's timing module, a quartz oscillator is locked to the incoming timing signal throughout normal operation. During periods when a valid signal is not available, the oscillator operates in a less disciplined condition known as holdover. In the latter case, a quartz oscillator must remain well-behaved to minimize system phase error.

Figure 1 depicts the fundamental elements of a phase locked loop system. During locked conditions, the reference signal's frequency characteristics are effectively low-pass filtered with a cut-off frequency dictated by the bandwidth of the control loop. Conversely, the output of the quartz oscillator is high-pass filtered with the same bandwidth constraints. Thus any tendency for the quartz oscillator to drift in response to temperature variation, component aging, random walk noise or small spontaneous frequency jumps is negated, within the limits of the loop's time constant, by the servo. Drift cannot be entirely mitigated during periods of holdover, which is an operational state in the absence of an external timing signal where the control loop effects frequency correction using recently observed oscillator behavior. The greatest risk of phase build-up occurs when the

quartz oscillator is free-running in an entirely autonomous manner.

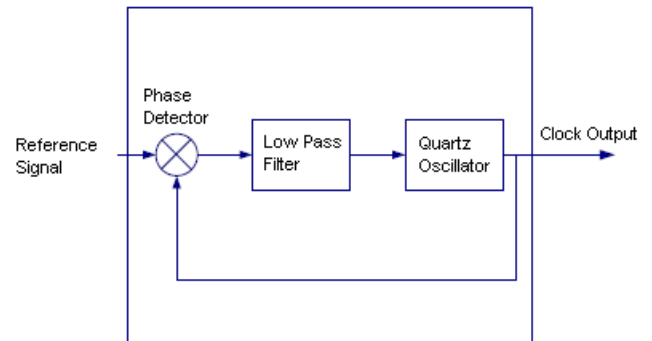


**Figure 1** Basic PLL Diagram

System designers must be cognizant of factors that create conditions around the quartz oscillator that mimic temperature changes, since the resultant frequency perturbations compound the accumulation of phase error during holdover. One often overlooked factor is airflow. A change in airflow around the oscillator enclosure is, in effect, equivalent to an ambient temperature change. An airflow change may occur as a result of cycling or variable-speed cooling fans within the system. The effects from airflow on various aspects of oscillator frequency stability and drift will be reviewed.

## II. Phase Error Free-Run

During holdover or free-run, sources of significant accumulated phase error at the oscillator level include initial phase offset ( $x_0$ ), frequency drift (D) and relevant stochastic noise processes ( $\epsilon(t)$ ) including random walk frequency modulation (RWFM). Equation (1) relates phase error between the oscillator and reference signal to these parameters, and is a generalization of the equation reported by Allan. [1]

$$x(t) = x_0 + \sum_{i=0}^m \frac{D_i \cdot t^{i+1}}{i+1} + \epsilon(t) \quad (1)$$

Coefficients  $D_i$  characterize the initial frequency offset ( $D_0$ ), linear drift ( $D_1$ ), as well as higher order drift terms.  $D_i$  reflects frequency variation caused by, among other factors, aging, warm-up and temperature variations. Drift rates can vary over time necessitating a piecewise approximation of phase error.

### III. Phase Error Closed-Loop

Equation (1) is also applicable during normal operation when the quartz oscillator is locked to the network reference. However,  $D_i$  observed at the timing network's output will reflect that of the reference, and thus is much lower than that achievable with the free running oscillator.

During lock, the linear drift component is attenuated to near zero while stochastic noise and/ or high rate frequency excursions become dominant. The loop bandwidth dictates which stochastic noise processes are important. Smaller loop bandwidths correspond to longer loop time constants, effectively increasing the significance of oscillator noise contributions close to carrier and of high-rate frequency changes. With large bandwidths, white phase and flicker phase are passed through the loop. As the loop bandwidth is decreased, white frequency and flicker frequency become a concern. With very tight bandwidths, a larger amount of the quartz oscillator's RWFM noise is passed to the timing network's output.

Figure 2 reveals the significance of loop bandwidth on accumulated phase error resulting from stochastic noise. In this example, RWFM and flicker FM noise processes dominate during the relevant observation time. When the update rate is quite low, such as for a loop bandwidth of 0.001 mHz, there is relatively little improvement in phase error. In contrast, a faster update rate afforded by a loop bandwidth of 1 mHz yields a much smaller phase build-up over the measurement time period.

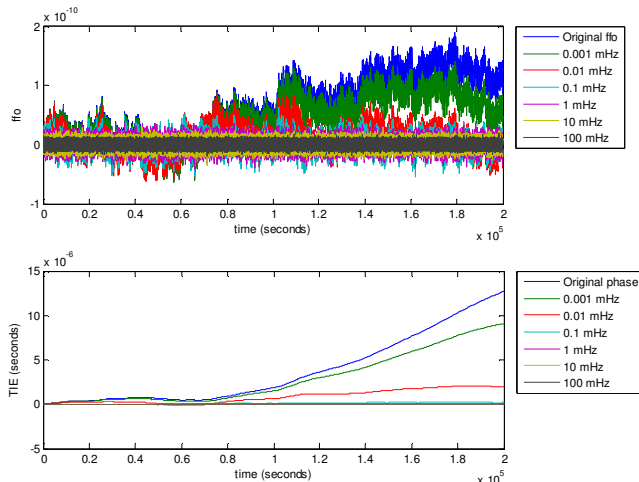


**Figure 2** Phase error as a function of loop bandwidth

### IV. Short-term Stability Constant Airflow

The authors have demonstrated that the Allan deviation (ADEV) of many ovenized oscillators subjected to constant airflow shows improvement over measurements taken in still air. Major design factors influencing this behavior are package hermeticity and internal insulating material.

During airflow testing, a small computer cooling fan was placed roughly six inches from the device under test. The fan was powered continuously during constant airflow testing or switched on and off at a constant rate during cycled airflow testing. Volumetric airflow was about 15 cubic feet per minute.

The ADEV results of a high stability OXCO measured during both constant airflow and in still air is shown in Figure 3. The short-term stability is substantially improved during exposure to airflow. In some circumstances, a similar improvement of ADEV is possible in still air by installing a tightly fitting cover over the unit.

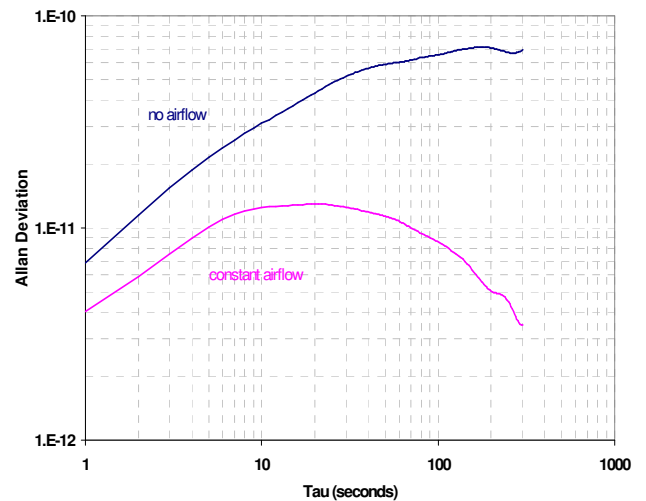


**Figure 3** ADEV comparison in still and moving air

### V. Phase Error Constant Airflow

ADEV computations for fractional frequency datasets generated using a specific combination of power law noise (including RWFM) show very similar slope and magnitude characteristics. In contrast, the same datasets yield a wide range of accumulated phase error. This becomes a major concern to telecom engineers when the dominant stochastic noise process is RWFM, since the measured phase error over equal time intervals may vary significantly.

Referring to the ADEV results in Section IV, the RWFM is roughly  $4e-12$  per second during constant airflow and about  $7e-12$  per second in still air. Numerous phase accumulation datasets generated using these two levels of RWFM are graphed in Figure 4. The phase boundaries widen with increasing

RWFM levels. Nonetheless, it is statistically likely that, for a finite observation time, a smaller phase buildup could occur for a RWFM of  $7e-12$  per second (red traces) than for  $4e-12$  per second (blue traces).

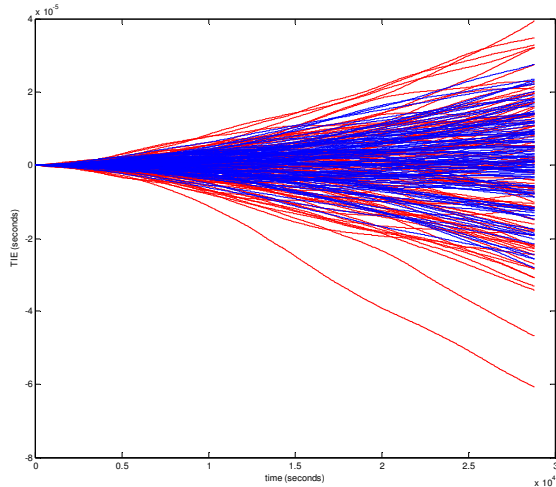


**Figure 4** Phase error, RWFM =  $4e-12/s$  and  $7e-12/s$

As a consequence, unless many phase error samples are taken, the improvement in short-term stability afforded by constant airflow may not be fully realized during a phase build-up analysis.

### VI. Phase Error Due to Frequency Shifts

Dynamic airflow will be shown to have a negative impact on OCXO stability. First though, consider how periodic modulation affects accumulated phase. In Figure 5, fractional frequency data is modulated by a periodic perturbation resulting in symmetrical frequency shifts about a zero frequency offset.

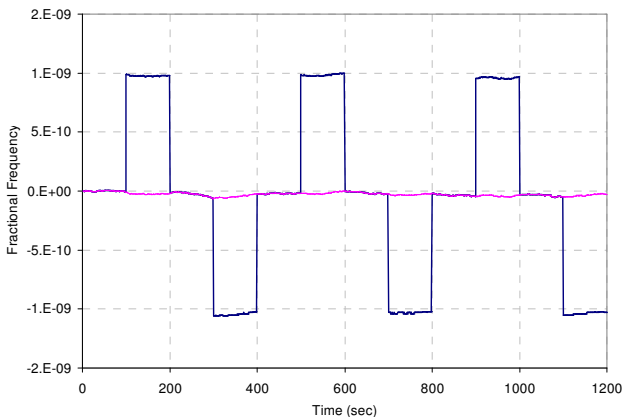


**Figure 5** Periodic modulation of fractional frequency data

The associated phase build-up computed for both datasets is shown in Figure 6. The magenta trace represents the unperturbed phase response over a 20 minute time period. The blue trace describes how phase relates to periodic frequency shifts. Note that the ending phase is  $-32.5$  ns in both cases. A zero net

change in phase occurs when frequency jumps are symmetrical around the reference frequency.

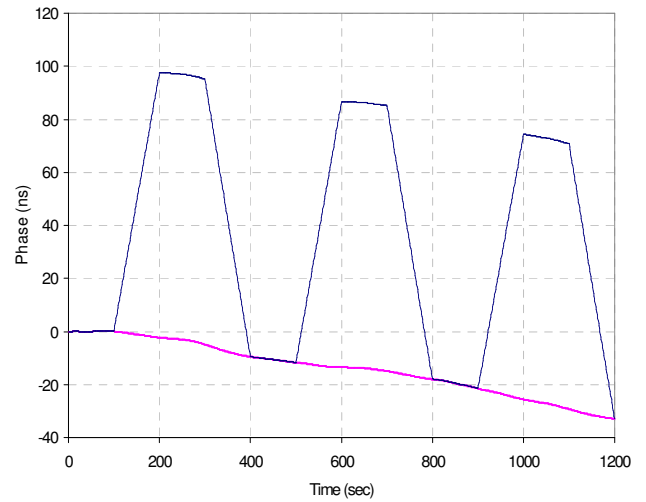


**Figure 6** Accumulated phase with modulation

### VII. Phase Error Dynamic Airflow

Figure 7 shows the frequency response of an OCXO exposed to intermittent airflow over a 10 kilo-second time period. In the zoomed view, note that the shape of each cycle varies and is asymmetric about both the time and frequency axes. This is due in part to oven controller instability, fluctuations in air dynamics, and quartz resonator hysteresis. The resultant asymmetry and the fact that the offset frequency is typically not zero causes phase build-up to increase very quickly as shown in Figure 8.

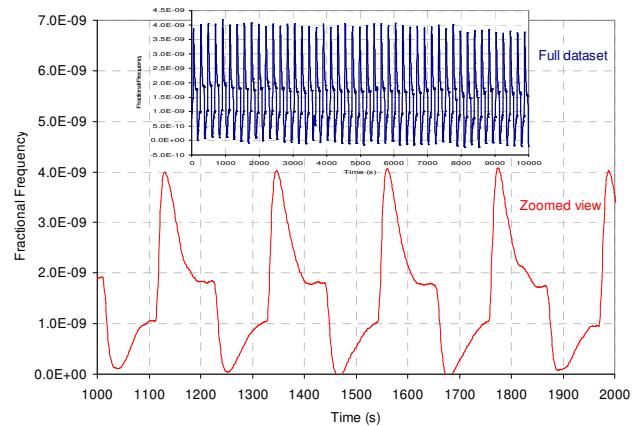


**Figure 7** OCXO frequency response to on-off airflow

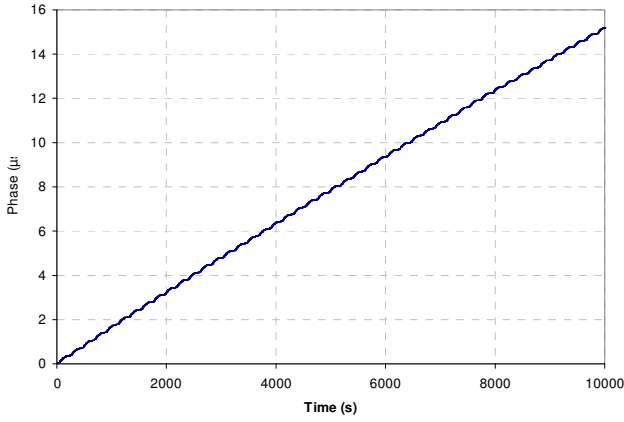


**Figure 8** Phase accumulation due to cycled airflow

### VIII. ADEV Dynamic Airflow

Allan deviation computed for the 10 kilo-second dataset from Section VII is shown in Figure 9.

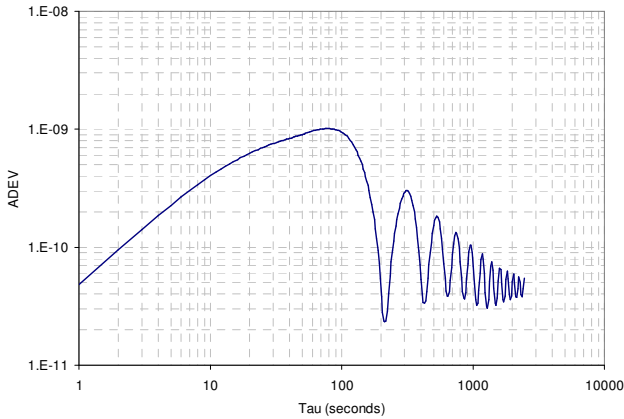


**Figure 9** Allan deviation for cycled airflow

The peaks and valleys evident in Figure 9 result from frequency modulation induced by the cycled airflow. The first valley's tau corresponds to the cycle period, which in this example is 200 seconds.

Equation (2) represents ADEV behavior during periodic cycled airflow, and is a variation of the modulation equation given by Allan. [2]

$$\sigma_y = \frac{S \cdot X_p}{\pi \cdot f_m \cdot \tau} \cdot \sin^2(\pi \cdot f_m \cdot \tau) \quad (2)$$

The frequency of the modulating airflow is  $f_m$  (Hertz),  $\tau$  is the observation time (seconds),  $X_p$  is the mass flow rate of air around the oscillator enclosure (grams per second), and  $S$  is the sensitivity of the oscillator to changes in mass flow (parts · second per gram). Keep in mind that the value of  $S$  is dependent upon the air temperature and may also vary with the angle that airflow is directed at the enclosure.

### IX. Phase Error Dynamic Airflow Closed-Loop

While locked to a more stable reference, the OCXO acquires the frequency stability characteristics of the reference for time constants below the loop bandwidth. Accordingly, the loop passes the frequency instability of the OCXO in a high-pass fashion. Applying various loop bandwidths to the frequency data in Section VII yields the family of curves shown in Figure 10. Analogous to that shown for the stochastic noise example in Section III, loops with shorter time constants are more effective at filtering abrupt frequency changes.

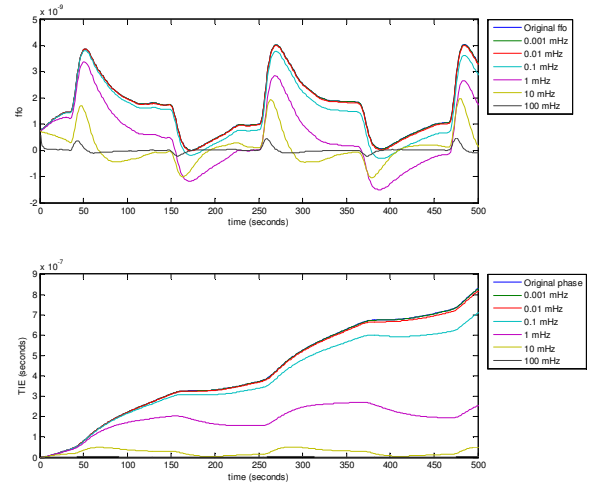


**Figure 10** Frequency and phase error vs. loop bandwidth

### X. Mitigating Airflow Impact

Designers can use techniques that reduce the impact of intermittent airflow on an oscillator's frequency stability. Two common options are placing a barrier between the airflow source and the oscillator, or placing an auxiliary cover over the unit. However, there are certain thermally related drawbacks associated with placing a cover over an OCXO, such as offsetting the oscillator enclosure temperature.

Figure 11 shows the differences in the frequency response of a 1 inch square hermetic OCXO exposed to cycled airflow with and without an auxiliary cover. The calculated ADEV of each dataset is shown in Figure 12, where it is apparent that a cover has increased the stability at all computed taus.

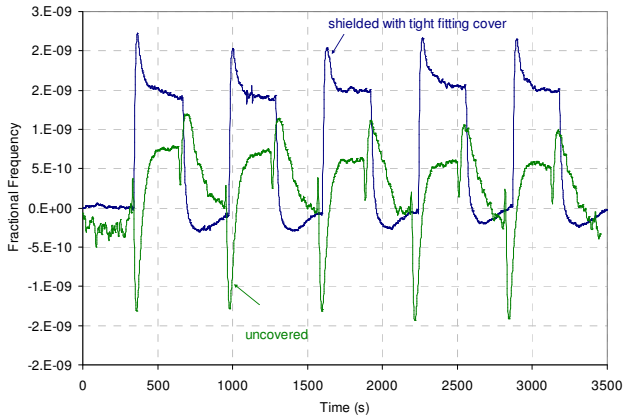


**Figure 11** Frequency with and without a cover (1 inch<sup>2</sup>)

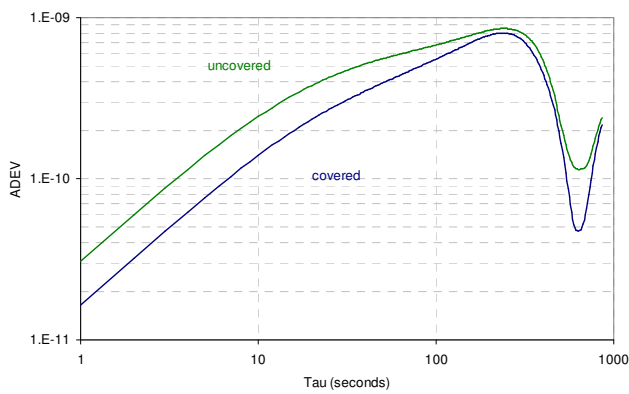


**Figure 12** ADEV with and without a cover (1 inch<sup>2</sup>)

The two frequency datasets are then converted to phase error and plotted in Figure 13. Although the short-term stability improved as previously mentioned, the phase error dramatically increased with the inclusion of a cover.

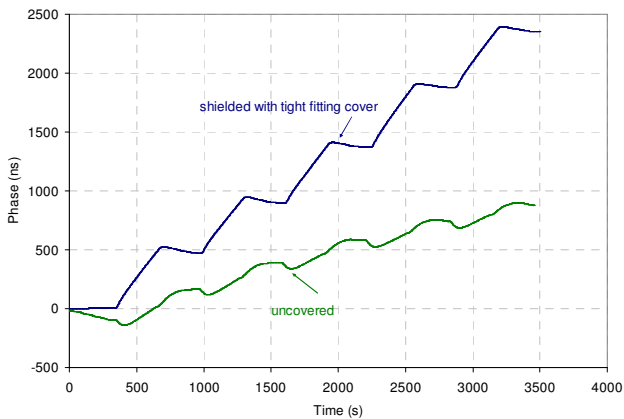


**Figure 13** Phase error with and without a cover (1 inch<sup>2</sup>)

In a second example, a 9x14 OCXO was subjected to the same manner of cycled airflow. As shown in Figure 14, the frequency response to cycled airflow has been completely altered. Based on the results in Figure 15, the use of an auxiliary cover improved the

ADEV. Likewise, as shown in Figure 16, the accumulated phase error has shown improvement.

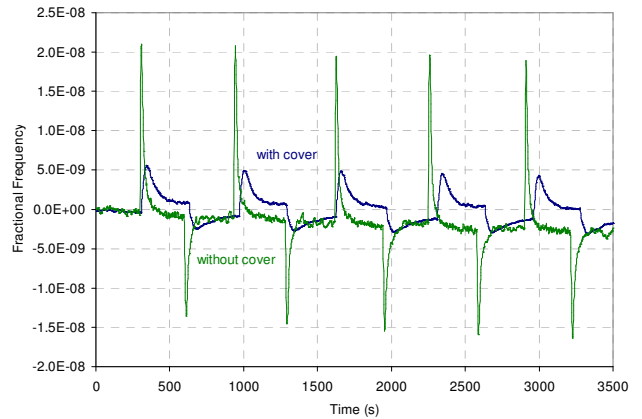


**Figure 14** Frequency with and without a cover (9x14)

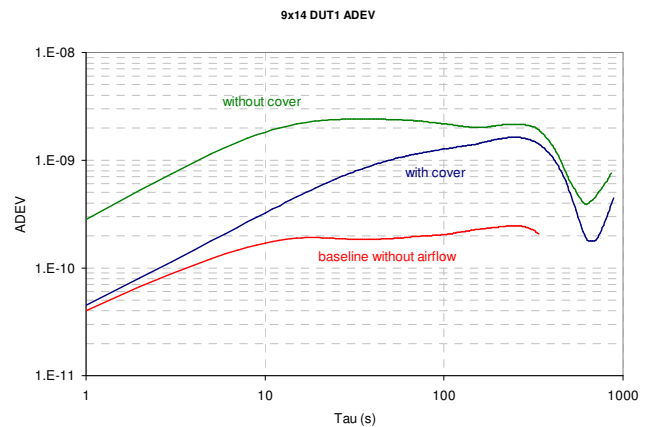


**Figure 15** ADEV with and without a cover (9x14)

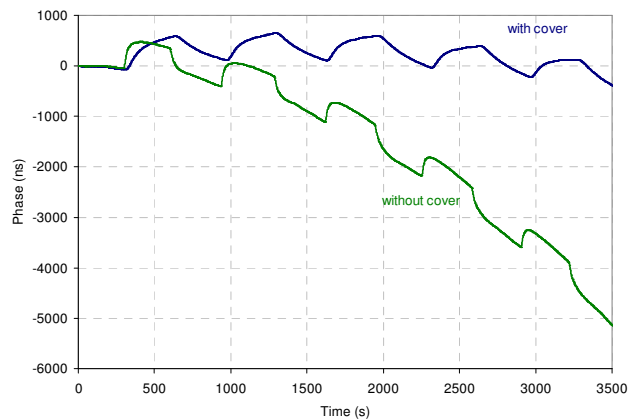


**Figure 16** Phase error with and without a cover (9x14)

These two designs respond differently with the addition of a secondary cover. Though the cycle-to-cycle asymmetry can influence phase error, as shown in Section V, variability of the phase error due to RWFM may account for some of the discrepancy.

## XI. Phase Error Due to Aging Rate Change

Exposing an OCXO to ambient temperature variation may result in more than just an abrupt frequency shift. The authors have found that it is not uncommon to observe a change in the medium to long term frequency drift of an OCXO following a temperature change, or in this context, an alteration in the airflow. Referring to Figure 17, the blue trace represents the stabilized frequency of an SC cut OCXO. The frequency response characterized by the magenta trace occurred following exposure of the same OCXO to numerous on/off airflow cycles. The linear rate of frequency change over a 10 kilo-second observation time increased in magnitude from  $-0.43$  ppb/day to  $-2.2$  ppb/day. Correspondingly, the phase error increased as shown in Figure 18. Hence, the aging trend established during normal operation in the absence of airflow and then applied during holdover with cycled airflow may yield inadequate aging compensation.

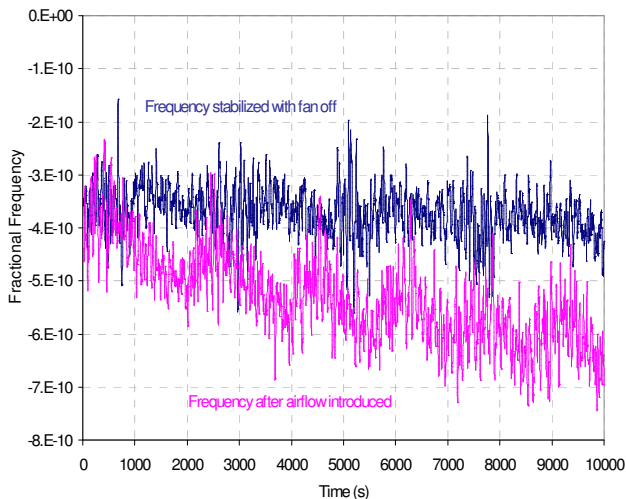


**Figure 17** Frequency response following airflow change

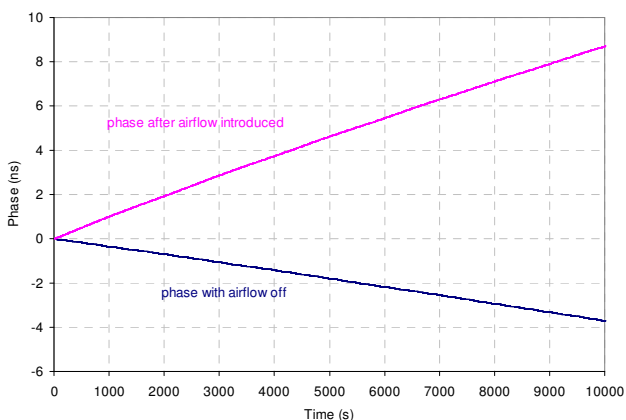


**Figure 18** Change of phase error following induced airflow

## XII. Conclusion and Summary

We have built upon previous work that analyzed the influence of environmental perturbations on the short-term stability of an oscillator to now look at the influence on the accumulation of phase error in a signal derived from such an oscillator. In our experiments and analyses, we examined the mitigating effects of operating an oscillator closed loop in a PLL or tracking loop on both internal (noise driven) and external (environment driven) perturbations. We also examined some approaches to mitigating the effect of airflow on an oscillator and found that while general conclusions can be drawn about the influence on short-term stability the same can not be said for phase accumulation.

If one is attempting to predict the influence that the environment will have on phase accumulation, it is vital to understand how the candidate oscillator will interact with both the loop dynamics of the host system and the environment as a whole.

### Acknowledgement

The authors express gratitude to Bill Holbrook for creating the accompanying poster.

### References

[1] Allan, David W., "Time and Frequency (Time-Domain) Characterization, Estimation, and Prediction of Precision Clocks and Oscillators", IEEE Transactions on Ultrasonics, Ferroelectrics, and Frequency Control, Volume UFFC-34, No. 6, November 1987

[2] Ibid